New Aspects on Melting and Annealing Behaviour of Polymers

J. Haase, S. Köhler, and R. Hosemann

Fritz-Haber-Institut der Max-Planck-Gesellschaft, Teilinstitut für Strukturforschung, Berlin-Dahlem

Z. Naturforsch. **33a**, 1472–1483 (1978); received August 12, 1978

Poly(1-butene) (PB) crystallizes from the melt in a metastable modification II (mod. II) which slowly transforms into the stable modification I (mod. I). X-ray wide angle (WAXS) measurements show that in mod. I the size of the microparacrystallites (mPC's) in chain direction, $\overline{D}_{012}$, the polydispersity g_D of the size distribution in this direction, the lateral size $\overline{D}_{110}$ and the paracrystalline g_{110}-value do not change upon annealing at temperatures up to the melting point. In mod. II, however, the sizes $\overline{D}_{012}$ and $\overline{D}_{110}$ increase with rising annealing temperature T_{ann}. At a certain T_{ann} and beyond a sufficient annealing time t_{ann} the size $\overline{D}_{012}$ shows a logarithmic increase with t_{ann} whereas $\overline{D}_{110}$ stays constant. Measuring melting points T_m of mod. I-samples, we found a linear relationship between T_m and $1/\overline{D}_{012}$ according to the Thomson equation resulting in a melting point for an infinite crystal of T_m^∞ (mod. I) = 139 °C and a mean surface free energy of $\overline{\sigma_e'}$ (mod. I) = 47 ergs/cm². T_m versus $1/\overline{D}_{012}$ for mod. II is linear only for high $\overline{D}_{012}$-values yielding T_m^∞ (mod. II) = 130 °C and $\overline{\sigma_e'}$ (mod. II) = 29 ergs/cm². However, a partially molten and afterwards quenched sample of mod. I with small mPC's shows a mod. II-peak which fits the straight line extrapolated from the large $\overline{D}_{012}$-values. The DTA curves of mod. I-samples shift to higher temperatures and narrow after annealing although the crystallite sizes and size distributions remain as well as the paracrystalline distortions the same.

X-ray and DTA measurements eliminate therefore surface premelting and selective melting of thinner and more distorted lamellae in mod. I. Upon annealing this modification, $\overline{\sigma_e'}$ decreases from 47 ergs/cm² to 15 ergs/cm² and the distribution of σ_e' narrows. The latter determines predominantly the shape of the DTA curve. The Thomson equation therefore, applied to different samples links only the average crystallite size and the mean surface free energy with the melting point. In mod. I partial melting occurs independent of $\overline{D}_{012}$ and starts mainly at those mPC's which have exposed surfaces with high σ_e'. At the beginning only single mPC's or single lamellae melt, but no bundles of lamellae. The logarithmic increase of $\overline{D}_{012}$ in mod. II with t_{ann} can be explained according to Hosemann's model of "lateral melting" also by a partial melting of mPC's with unprotected lateral surfaces and by a consecutive solid state diffusion of their chainsegments into the two mPC's adjacent in chain direction, increasing the averaged sizes of the long period and the lamellae thickness.

Introduction

Although a variety of measurements on semicrystalline polymers have been done with different physical methods, neither the growth of the crystals on annealing nor their melting is a thoroughly understood process. For both phenomena which generally overlap and partly depend on each other several different mechanisms have been proposed.

Mainly two mechanisms seem to contribute to the growth of the crystals which in literature is often called lamellar thickening, because laterally infinite crystalline lamellae are erroneously assumed: On one hand selective melting of thinner [1] or more distorted [2] lamellae with successive recrystallization to thicker ones is supposed and a solid state diffusion (refolding) [3] on the other.

Again two different theories have been presented to explain the melting process. As already mentioned above, melting is thought to be selective [1]: Lamellae should melt according to their distribution of thicknesses which must consequently manifest itself in the shape of the corresponding DTA curve [4]. Competing with this explanation of the melting process is the surface premelting model [5] which interprets the continuous decrease of the crystallinity with rising temperature in the melting range es enlargement of the fold surface layer at the expense of either the crystallite size in chain direction or the lateral extension of the crystal. The surface premelting model was postulated to understand the intensity changes in the X-ray small angle (SAXS) pattern on annealing of semicrystalline polymers. However, it is successful only for samples with crystallinities $\alpha > 50\%$ [6].

A quite different approach to explain the whole of the annealing and melting phenomena has already been published in 1962 by Hosemann [7] and is characterized by "lateral melting". The lamellae consist of mosaic blocks with paracrystalline lattice distortions and therefore are called microparacrystallites (mPC's). Their lateral

grain boundaries are of outstanding importance as they are preferentially attacked if unprotected from neighbouring mPC's. Lamellar thickening can be accomplished by destroying the mPC's mainly at the ends of lamellae and by simultaneous refolding of the mPC's of neighbouring lamellae into these regions. Accordingly the melting process will start at exposed mPC's which occur not only at the ends of lamellae, but also within them at locations where the correlation of the sites of neighbouring mPC's is small [6].

In this paper WAXS investigations supplemented by calorimetric measurements (DTA) on melt-crystallized isotactic PB are dealt with, which give a deeper insight into the annealing and melting behavior at least of this special polymer and lead to surprising results which cannot be explained by the conventional concepts of selective melting and surface premelting. PB was chosen because of two reasons. Firstly it is possible to calculate directly the crystallite size in chain direction from the WAXS pattern of PB in contrast to meltcrystallized polyethylene (PE). Secondly PB is of special interest because samples of mod. I do not show any change of the mean lamellar thickness on annealing a temperatures up to melting point [8]. On account of this extraordinary behaviour, a clear analysis of the melting process is successfull for the first time.

Experimental Part

1. Samples

All measurements were performed with isotactic PB of molecular weight $M_v = 2.3 \cdot 10^6$ of the Chemische Werke Hüls AG *. PB foils were melted between thin sheets of brass for 15 min at 180 °C and afterwards quenched in water of 20 °C. By this means mod. II crystallizes.

Mod. II slowly transforms into the stable mod. I. The transformation is quickened by applying longitudinal stress [9]. The half-life of mod. II is temperature-dependent and has at 20 °C a minimum of the order of 1 d [10, 11]; it increases rapidly with rising temperatures. After storing mod. II for one week at $T \geqq 100$ °C practically no mod. I had formed. Moreover, the half-life of mod. II is dependent on the morphology of the sample [12]. The transformation is a solid-solid one which proceeds without change of crystallinity [13]. In Table 1 some characteristic data [14, 15] of both modifications are listed. As may be seen from Table 1, the 11/3-helix of mod. II with a distance between consecutive monomers in chain direction of 1.87 Å changes by the transformation into the 3/1-helix of mod. I with a corresponding distance between monomers of 2.17 Å. Therefore, the transformation may be formally described as stretching of a helix in the longitudinal direction. As the crystallinity stays constant, we conclude that no segments of the molecules change from the crystalline to the amorphous phase and vice versa so that the crystallite size in chain direction also changes by about 15%. This cannot be proved directly by X-rays, because the WAXS pattern of an isotropic sample of mod. II has no measureable reflection which gives the crystallite size in chain direction. SAXS diagrams, taken before and after the transformation reveal a long period increase of $(14 \pm 5\%)$. However, because of the small difference in electron density between the crystalline and amorphous phase — $\varrho_a = 0.87$ g/cm³ [15] —, it is difficult to measure the long period of mod. II, exactly. As the density increase reveals (cf. Table 1), the polymer chains draw closer by transformation. Obviously, this prevents a thickening of the lamellae of mod. I by solid state diffusion.

Table 1. Characteristic data of poly(1-butene), mod. I and II [14, 15].

	Mod. II	Mod. I
Crystal system	tetragonal	hexagonal
Lattice constant c [Å]	20.6	6.5
Helix (u/t)	11/3	3/1
Helical parameter $p(=c/u)$ [Å]	1.87	2.17
Cryst. density [g cm^{-3}]	0.90	0.95
Equilibr. melting point [°C]	130	138

Assuming constant crystallinity, from the density increase (cf. Table 1) and the increase of the crystallite size in chain direction by about 15%, a decrease of the lateral crystallite sizes by about 10% is calculated. Therefore, an isotropic sample should undergo a shortening of about 0.5%, as has been measured [9]. Therefore, if the crystallite sizes of either mod. I or II are known, then the sizes of the other can be calculated immediately. In the present paper only crystallite sizes of mod. I were measured, because mod. II has a limited lifetime and no measurable reflection giving the crystallite size in chain direction.

* Thanks are due to Dr. G. Goldbach for supplying the samples.

Immediately after quenching to 20 °C, the PB samples were annealed for different times at different temperatures. During the short time at 20 °C, measurable transformation from mod. II to I did not occur in any of the samples. Moreover, at the annealing temperatures, the transformation was always so slow that mod. II-crystallites could grow corresponding to the annealing temperature and time, without being disturbed by the transformation. After annealing, the samples were quenched again to 20 °C. Two samples have been analysed in more detail: Sample A — quenched and sample B — quenched and annealed in mod. II for 10^3 min at 111 °C.

DTA and DSC measurements were made before (i.e. in mod. II) as well as after the transformation into mod. I. WAXS patterns, on the other hand, were taken only after the transformation, when the remaining percentage of mod. II was less than 10%. Some of the mod. I-samples were annealed again (i.e. now in mod. I) and afterwards quenched to 20 °C likewise.

2. *Techniques*

DTA and DSC

The DTA curves were taken in a microcalorimeter MCB with a heating rate of 2 °C/min. The peak temperatures are defined as melting points T_m. Heats of fusion were measured after calibrating the calorimeter with benzil. A heat of fusion for the fully crystalline mod. I of $\Delta h_f = 1675$ cal/monomer unit = 29.9 cal/g [16] was used for crystallinity calculations. Moreover, a Perkin-Elmer calorimeter was available for supplementary DSC measurements* with a maximum heating rate of 32 °C/min.

WAXS and SAXS

WAXS patterns were taken in precision Guinier cameras (AEG, Huber) with Johansson monochromator using $CuK\alpha_1$-radiation. The measured line widths were corrected with $CaWO_4$ samples for instrumental broadening. Film as well as counter methods were used, the former for measuring integral widths, the latter mainly for evaluating the line profiles. A heatable sample holder designed by Schmidt [17] was available, which guaranteed a temperature constancy of ± 0.3 °C within the sample.

Supplementary SAXS investigations were made in a Kiessig camera with point collimation. From WAXS of mod. I the reflections 110, 220 and 012 were evaluated. It had been shown before [18] that in the direction perpendicular to the netplane (110) paracrystalline distortions occur, so that from the integral width δb of the reflections 110 and 220 the mean crystallite size $\bar{D}_{110}$ and the paracrystalline g_{110}-value can be calculated according to

$$\delta b = \frac{1}{D} \oplus \frac{\pi^2 g^2 p^2}{d} \tag{1}$$

where d is the spacing of the scattering netplanes and p the order of the WAXS reflection. The linkage $\oplus$ between the crystallite size term and the distortion term in Eq. (1) is dependent on the profile of the lattice factor and shape factor [19]. As there is only an angle of 12° between the normal to the netplane (012) and the chain direction, D_{012} is a good approximation of the crystallite size in chain direction (= c-axis). $\bar{D}_{012}$ is directly calculated from $\delta b_{012} = 1/\bar{D}_{012}$ neglecting the distortion term. However, from the empirical relation [20]

$$\alpha^* = gN^{1/2} \quad \text{with} \quad \alpha^* \cong 0.1; \quad N = D/d\,. \tag{2}$$

and Eq. (1) it can be estimated that the error is only about 10% independent of the g-value. In the present paper, the changes in $\bar{D}_{012}$ are of main interest, so that the simplification is of no importance. Moreover, measuring the widths of the 202 and 404 reflections, we found no distortions in this direction which is tilted against the c-axis by about 23°. Distortions in chain direction, therefore, probably do not occur. From the profile of the 012-reflection, the crystallite size mass-distribution $M(D)$ in chain direction is calculated, which is defined by its polydispersity g_D [21]. In this method a distribution of Maxwellian type is assumed

$$M(D) \sim (D/c)^n \cdot e^{-(D/c)^2}; \qquad D = c(n+1)/(2n+3)^{1/2} \tag{3}$$

the exponent n of which is related with the polydispersity g_D by

$$g_D =_{\text{def.}} (\overline{D^2}/\bar{D}^2 - 1)^{1/2} = (2n+2)^{-1/2}\,. \tag{4}$$

n is calculated by fitting the experimental profiles with analytical functions of the type

$$i(b) \sim \{1 + k^2(b - b_r)^2\}^{-(n/2+2)} \tag{5}$$

* Thanks are due to Dr. F. Asmussen for performing the DSC measurements.

where $i(b)$ is the intensity, b the absolute value of the scattering vector in reciprocal space and b_r that of the reflection maximum.

$$b = 2 \sin \vartheta/\lambda; \quad k = 2\pi c/\sqrt{5}\,.$$

Results and Discussion

1. Modification I

Melting Points

In Fig. 1 melting points T_m of mod. I-samples are plotted versus the reciprocal of the crystallite size in chain direction $1/\bar{D}_{012}$ (solid line). The widely spread $\bar{D}_{012}$-values originate from annealing of quenched samples in mod. II at different temperatures. The excellent linear relationship in Fig. 1 is explained according to the one-dimensional so called Thomson-Equation [22]

$$T_m = T_m^\infty (1 - 2\overline{\sigma_e}/\Delta h_f \cdot \bar{D}_{012}) \qquad (6)$$

in which T_m^∞ is the melting point of an infinitely large crystal with a heat of fusion Δh_f. $\overline{\sigma_e}$ is the surface free energy of the lamellae of thickness $\bar{D}_{012}$ which is mainly given by the fold surface free energy. Equation (6) is derived from the melting point formula for a chain folded mPC of fold length l and of lateral dimensions a and b having a fold surface free energy σ_e and a lateral surface free energy σ, as follows

$$T_m = T_m^\infty (1 - 2\sigma_e/\Delta h_f l - 2\sigma/\Delta h_f a - 2\sigma/\Delta h_f b)\,. \qquad (7)$$

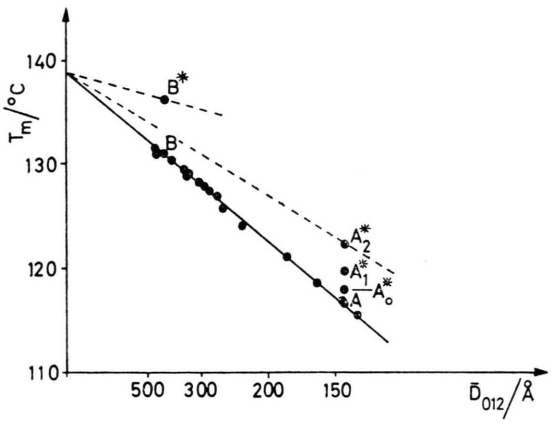

Fig. 1. Peak melting points of poly(1-butene) samples in mod. I vs. the reciprocal mean crystallite size in chain direction; line A—B: samples annealed in mod. II; A_0*, A_1*, A_2*, B*: samples A and B annealed in mod. I (cf. Table 4 and text).

This formula can be expanded further by a term describing the melting point depression by lattice distortions [2]. If $\sigma_e \gg \sigma$ or / and $a, b \gg l$ then Eq. (6) holds with $\overline{\sigma_e} = \sigma_e$ (and $\bar{D}_{012} = l$). Otherwise σ_e is smaller than $\overline{\sigma_e}$, i.e. the lateral surface free energy contributes to the lowering of the melting point. In the present case this possibility could not be ruled out. From Fig. 1 and Eq. (6) results a melting point $T_m = (138.6 \pm 0.5\,°C)$ in good agreement with the value given in the literature [15] and a surface free energy of $\overline{\sigma_e} = 47$ ergs/cm^2.

Crystal Growth

Figure 1 is different from corresponding diagrams of other semicrystalline polymers which deviate more or less from a straight line, if recorded with an equally low heating rate (2 °C/min) [5]. This behaviour is explained by a thickening especially of small lamellae during the heating in the DTA apparatus. Mod. I obviously does not behave so. This unusual result has been established by annealing of many different samples: Upon annealing at temperatures up to the melting point and measuring at the annealing temperature, the crystallite size in chain direction $\bar{D}_{012}$ does not change within an experimental error of less than $\pm 5\%$. An example is given in Table 2 where the results for sample B are plotted which had been annealed in mod. II for 10^3 min at 111 °C (cf. Figs. 1 and 8).

Sample B was brought successively to the temperatures listed in column 1 of Table 2 and measured at these temperatures after being maintained there for approximately 24 hours. From integral reflection intensities the molten percentage of mod. I was calculated (cf. column 2 in Table 2).

Table 2. Mean crystallite size in chain direction, $\bar{D}_{012}$, the polydispersity of the crystallite size mass-distribution in this direction, g_D, the mean crystallite size in a lateral direction, $\bar{D}_{110}$, and the paracrystalline g_{110}-value during melting of poly(1-butene), mod. I, sample B.

T	mod. I molten	$\bar{D}_{012}$	$g_D(012)$	$\bar{D}_{110}$	g_{110}
°C	%	Å		Å	%
20	0	412	0.37	740	2.4
125.0	0	426	0.37	640	1.8
131.0	41	420	0.37	780	2.2
132.0	63	422	0.38	660	1.8
132.5	78	429	(0.40)	680	2.1
133.0	88	(410)		710	2.0

Column 3 of Table 2 shows clearly that $\bar{D}_{012}$ remains the same even when nearly 90% of mod. I are molten. This behaviour is unknown to semicrystalline polymers till now. How can it be explained?

a) As already mentioned in connection with the density increase due to the transformation, no solid state diffusion occurs. The structure of mod. I must be fixed such that the chain mobility up to the melting point is not high enough to allow a snaking type of refolding of the chains.

b) A growth of the mPC's of mod. I by partial melting and recrystallization in the same modification is not possible, because only mod. II crystallizes from the melt. This result is already known from measurements of Powers et al. [23] as well as Vidotto et al. [24] who always observed recrystallization in mod. II although seeds of mod. I were present. Crystallization of mod. II starts at temperatures approximately below 115 °C (cf. Fig. 6 and text), so that at annealing temperatures $\geqq 115$ °C a molten part of PB remains permanently molten. At temperatures between 80 °C and 115 °C a molten percentage of mod. I recrystallizes in mod. II, but there is practically no transformation from mod. II to I (cf. experimental part). Therefore by measuring WAXS reflections at annealing temperatures $\geqq 80$ °C the results are always related to the nonmolten part of mod. I (cf. Table 2, column 2 and Table 4).

On principle, however, it is possible to change the mean crystallite size of a mod. I-sample indirectly by partial or total melting, recrystallization in mod. II and waiting till the transformation into mod. I is complete.

Melting Behaviour

The very fact that mod. I-crystallites do not thicken on annealing, meets the requirements for analysing the melting process and for proving existing theories.

If melting were selective with respect to the lamellar thickness [1] in such a way that according to Eq. (6) thin lamellae melt first followed by thicker ones at higher temperatures then the mean lamellar thickness should increase with rising temperature and the crystallite size distribution in chain direction defined by the polydispersity g_D should decrease. Accordingly, if melting were selective with respect to the lattice distortions, the paracrystalline g-value should decrease. However, this consideration only holds, when the surface free energy σ_e' is the same for all the different crystallite sizes within a sample (refer to section "Annealing effects"). The surface premelting model [5], on the other hand, predicts an increasing length of the fold loops with rising temperature. If this were accomplished by melting the mPC's from the fold surface inward to the core, then the mean crystallite size in chain direction, $\bar{D}_{012}$, should decrease. If, on the other hand, $\bar{D}_{012}$ remained constant, the mean lateral size should decrease. The results for sample B listed in Table 2 unequivocally prove that neither selective melting nor surface premelting occurs. During successive partial melting of mod. I up to about 90% not only the crystallite size in chain direction, $\bar{D}_{012}$, remains the same, but also the polydispersity g_D of the size distribution in this direction, the lateral crystallite size $\overline{D}_{110}$ and the paracrystalline g_{110}-value, the latter measuring the lattice distortions in the direction perpendicular to the netplane (110).

Quite similar results have been obtained for the quenched sample A with a mean crystallite size of about 200 Å.

The results in Table 2 cannot be explained as superposition and mutual compensation of the effects caused by selective melting and surface premelting. This is already shown by the constancy of g_D and furtheron established by measurements on another sample B, the WAXS pattern of which was taken alternatively at high and at room temperature. The results are listed in Table 3. It is seen clearly that $\bar{D}_{012}$ measured at high temperature is not smaller than that measured at room temperature. This eliminates conclusively surface premelting of mod. I in the sense of a partial melting of the

Table 3. Mean crystallite size in chain direction $\bar{D}_{012}$ of sample B of poly(1-butene), mod. I measured successively at high and at room temperature.

Temperature of measurement	mod. I [%] molten	$\bar{D}_{012}$ [Å]
125 °C	0	418
room temperature		400
128 °C	7	418
room temperature		424
131 °C	13	427
room temperature		420
133 °C	57	429
room temperature		405
135 °C	87	420

mPC's from the fold surface inward to the core. After quenching from 135 °C the 012 reflection of mod. I was strongly disturbed by reflections of mod. II present to about 87%, so that it could not be evaluated.

The finding is in agreement with results from Raman measurements on solution and melt-crystallized preannealed PE samples [25], where a constant crystallite thickness between room temperature and annealing temperature was obtained.

Now we focus our interest on the molten percentage of mod. I-samples upon annealing which after quenching recrystallizes in mod. II and if measured immediately after quenching, i.e. before the transformation from mod. II to I occurs, manifests itself in a mod. II-DTA peak separated from the mod. I-peak. When we start with sample A of known $\bar{D}_{012}$ which was quenched from the melt, melt it partially and quench it again, we know that

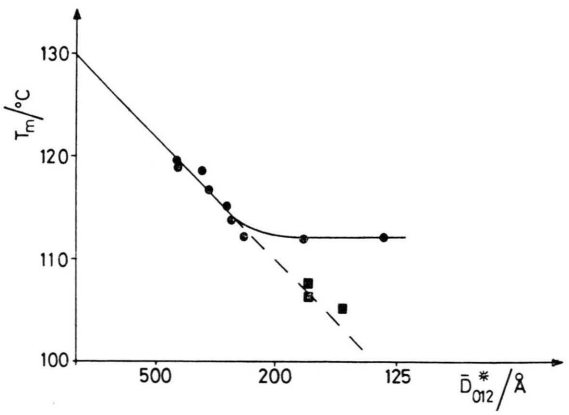

Fig. 2. Peak melting points of poly(1-butene) samples in mod. II vs. the reciprocal mean crystallite size in chain direction (full circles). The squares correspond to melting points of mod. II in samples which consisted of more than 90% of mod. I. The measured sizes $\bar{D}_{012}$ of mod. I were converted to corresponding sizes $\bar{D}^*_{012}$ (see text).

mPC's of the same size recrystallize in mod. II. Their melting points T_m are marked as squares in the diagram of T_m versus $1/\bar{D}_{012}$ for mod. II in Figure 2. The full circles in this diagram belong to samples which completely consisted of mod. II. They lie on the solid line which, extrapolated to high $\bar{D}_{012}$, gives $T_m = 130$ °C and which gets nearly horizontal for small $\bar{D}_{012}$. As mentioned above, the deviation from the straight line originates from a thickening of mod. II-crystallites during heating in the DTA apparatus.

The T_m-values of the partially molten samples fit in to the straight line extrapolated from high $\bar{D}_{012}$-values only if less than about 10% of mod. I was molten and recrystallized in mod. II on quenching. This result is of great importance: It proves that a thickening of mod. II-mPC's during heating in the DTA apparatus does not occur. Obviously, it does not occur, because the mod. II-mPC's are separated from each other in chain direction by mod. I-mPC's. Only single mPC's or single lamellae melt statistically, but no bundles of lamellae as supposed by Meyer and Kilian [4]. The result is in agreement with measurements of Petermann et al. [26] on PE, who found a melting of single mPC's preferentially at the ends of lamellae, but also within them [6]. The reason for this seems to be found in their exposed surfaces having a high surface free energy, as will be explained in the next chapter.

Annealing Effects

Although the mean crystallite size of mod. I-mPC's does not change, other quite interesting effects occur on annealing:

a) the melting point shifts to higher temperatures and
b) the DTA-curve narrows.

Table 4. Melting points T_m, DTA crystallinities α, mean surface free energies $\overline{\sigma_e}$ and some WAXS results of samples A and B of poly(1-butene), mod. I annealed for different times t_{ann} at different temperatures T_{ann} (cf. Figure 1).

Sample	T_{ann} [°C]	t_{ann} [h]	T_m [°C]	$\bar{D}_{012}$ [Å]	$g_D(012)$	$\bar{D}_{110}$ [Å]	g_{110} [%]	α [%]	$\overline{\sigma_e}$ [erg cm^{-2}]
A		0	116.8	146	0.16	378	1.9	36	47
A_0*	113	1	117.9	—	—	421	1.7	—	44
A_1*	113	10	119.8	—	—	—	—	—	40
A_2*	113	100	122.6	148	0.16	415	1.7	35	34
B		0	131.1	415	0.40	632	2.3	49	47
B*	varying	varying	136.3	not measured, but cf. Table 2 and text				48	15

The extent of these effects is dependent on the sample history on annealing temperature and time.

a) T_m-shift

Listed in Table 4 are the melting points of samples A and B, which were annealed for different times at different temperatures (samples $A_0^* - A_2^*$, B*). As crystallite sizes and lattice distortions do not change upon annealing, the T_m-shift can be explained according to the Thomson-Equation only by a decrease of $\overline{\sigma_e'}$ (cf. Table 4, column 9 and Figure 1). In the case of sample B the surface free energy decreases from 47 ergs/cm² to 15 ergs/cm² (sample B*). Similar results have been reported recently for isotactic polystyrene [27].

Changes in the fold surface are also indicated by SAXS measurements. As shown in Fig. 3, the long period reflection nearly disappears on annealing. It means that the electron density difference between the amorphous and the crystalline phase in the sample has decreased, i.e. that the density in the amorphous regions has increased.

b) Narrowing of DTA curves

The narrowing of DTA curves after annealing is seen in Fig. 4 (solid lines A, A_2^*, B and B*). It has been accepted quite generally in literature that the shape of the DTA curve reflects the crystallite size distribution in the sample [4, 22], so that a narrowing of DTA curves is explained as the narrowing of the size distributions. This explanation is wrong, at least for PB. This has been proved already by successive partial melting, where $\bar{D}_{012}$ and $\bar{D}_{110}$ stay constant. Moreover, the fact that the DTA curves narrow on annealing, although $\bar{D}_{012}$ and g_D remain constant, indicates again that their shape is not determined by the crystallite size distribution. In Fig. 4 not only the experimental DTA curves are drawn, but also theoretical ones (broken lines). The latter were calculated by giving each

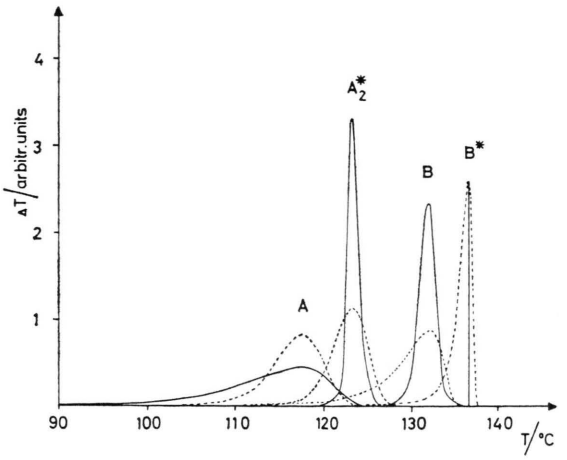

Fig. 4. DTA curves of different samples of poly(1-butene), mod. I (cf. Fig. 1 and Table 4); solid lines: experimental curves; broken lines: theoretical curves calculated from the crystallite size mass-distribution in chain direction (cf. Fig. 5) by means of the Thomson-Equation. The experimental curves of samples A_2^* and B have been refolded by the DTA instrument profile. The refolded curve of sample B* was omitted, because of its large error. Its location is indicated by a vertical line, its width δT should be smaller than 1 °C (cf. Table 5).

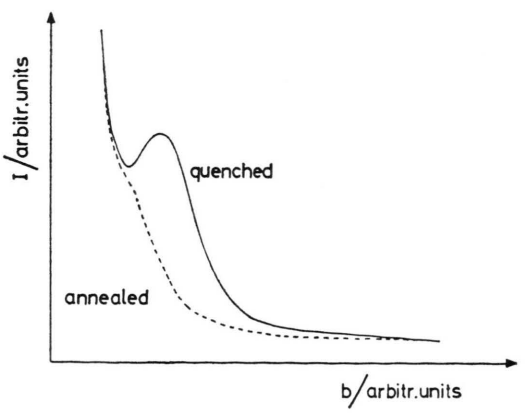

Fig. 3. Microdensitometer traces of SAXS patterns along the meridian of sample A before and after annealing in mod. I for 100 h at 113 °C (cf. Table 4).

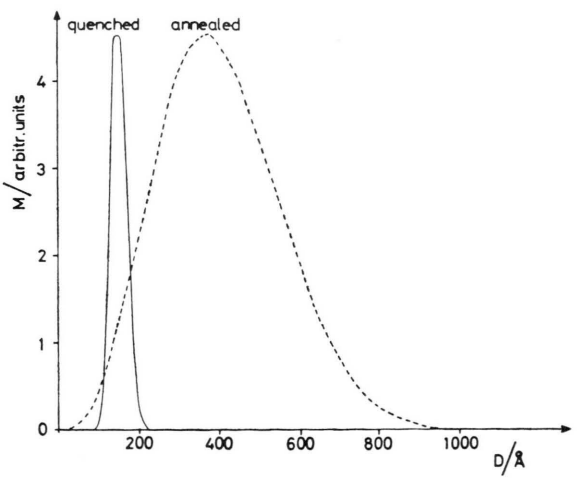

Fig. 5. Mass-distributions of the crystallite size in chain direction of samples A (quenched) and B (annealed in mod. II for 10^3 min at 111 °C) of poly(1-butene) calculated from Eqs. (3) to (5).

Table 5. Experimental and calculated widths δT of DTA curves, taken at half peak-height, for different samples of poly(1-butene), mod. I (cf. Figs. 1 and 4).

Sample	δT_{exp} [°C]	δT_{calc} [°C]
A	11.1	6.5
B	2.2	5.4
A_2*	1.5	4.5
B*	<1.0	1.8

individual crystallite size of the size distribution of Fig. 5, which was estimated from the 012 reflection profile according to Eqs. (3) to (5), a melting point according to the Thomson-Equation. For sample A and B a surface free energy of $\overline{\sigma_e'} = 47$ ergs/cm² were used, for the annealed samples values of $\overline{\sigma_e'} = 34$ ergs/cm² (sample A_2*) and $\overline{\sigma_e'} = 15$ ergs/cm² (sample B*), respectively. There is no agreement between experimental and theoretical curves. The experimental curve may be broader (curve A in Fig. 4) or sharper (curves A_2*, B, B* in Fig. 4) than the calculated one, as is also shown quantitatively by the corresponding half-widths listed in Table 5. Obviously, the Thomson-Equation with a constant σ_e' for all crystallite sizes within one sample cannot explain the experimental results. In addition to the size distribution there must be a distribution of the σ_e'-values so that altogether the distribution of the (σ_e'/D)-values determines the shape of the DTA curve. The Thomson-Equation applied to different samples, therefore, only links the mean crystallite size $\bar{D}$ and the mean surface free energy σ_e' with the melting point (cf. Equation (6)). The linear relationship between T_m and $1/\bar{D}_{012}$ for the unannealed samples (solid lines in Fig. 1) means that the mean value of σ_e' is the same for all samples.

Upon annealing of mod I.-samples σ_e' decreases and the distribution of σ_e' narrows.

The sample will melt first at those locations, where large (σ_e'/D)-values are present. Exposed (unprotected) surfaces have a higher σ_e'. This will happen predominantly at the ends of lamellae as there are exposed lateral and exposed fold surfaces. The importance of the lamellae ends for the annealing and melting process is underlined again by these findings. But also within lamellae, where the correlation of the sites of neighbouring mPC's sometimes is bad [28] so that unprotected surfaces result, melting may start. As mentioned above, these results are in good agreement with those obtained by electron microscopy [26].

2. *Modification II*

Melting Points

Melting points T_m of some samples of mod. II are plotted versus $1/\bar{D}_{012}$ in Fig. 2 (solid line) together with T_m-values of mod. II in samples which consisted of mod. II, only to about 10% (broken line). On extrapolating the linear part of the curve in Fig. 2, a melting point for an infinite crystal of $T_m^\infty = (130 \pm 1\,°C)$ is found in good agreement with other measurements [15]. Assuming Δh_f(mod. I) = 1675 cal/mol monomer unit [16], from the measured value Δh_r(mod. I)/Δh_f(mod. II) = 2.07 and from the crystalline density ϱ_e(mod. II) = 0.90 g/cm³ [15] a surface free energy of $\overline{\sigma_e'} = 29$ ergs/cm² results.

As already mentioned above, the deviation of the curve in Fig. 2 from a straight line points to a growth of the mPC's during heating in the DTA apparatus. This growth will be studied in detail in the next chapter.

Crystall Growth of mod. II

Except in one case which will be stated in Sect. c), in all following experiments the samples were quenched from the melt and annealed immediately after quenching, so that during this process practically no transformation into mod. I could occur. After annealing, the samples were quenched again and stored at room temperature long enough, so that now mod. II could transform completely into mod. I. The WAXS patterns were taken from mod. I because only this modification yields the crystallite size in chain direction. The values of $\bar{D}_{012}$, therefore, must be reduced by 15% and the values of $\bar{D}_{110}$ must be enlarged by 10% to get the corresponding ones for mod. II.

a) Crystal Growth as Function of the Annealing Temperature

In Fig. 6 the crystallite sizes $\bar{D}_{012}$ and $\bar{D}_{110}$ are plotted versus the annealing temperature T_{ann} for samples which were held at T_{ann} for 24 h and quenched afterwards to 20 °C. The crystallite size increases in chain direction by a factor of 2.5, laterally by a factor of 1.7 (maximum values). In contrast to stretched branched PE, where the mean shape of the mPC's remains the same [29], there does not exist an equilibrium shape for the mPC's of PB. Moreover, the growth of the mPC's in chain direction and laterally is not correlated. This is seen

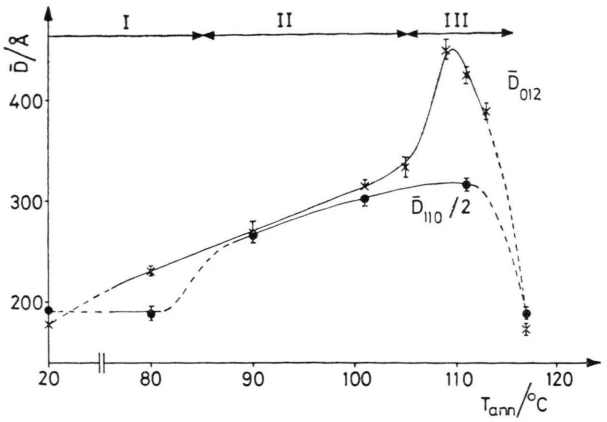

Fig. 6. Mean lateral crystallite size $\bar{D}_{110}$ and mean crystallite size in chain direction, $\bar{D}_{012}$, of annealed samples of poly(1-butene) vs. the annealing temperature measured at 20 °C. The annealing time was 24 h in all the cases. For the different temperature ranges I, II, III see text.

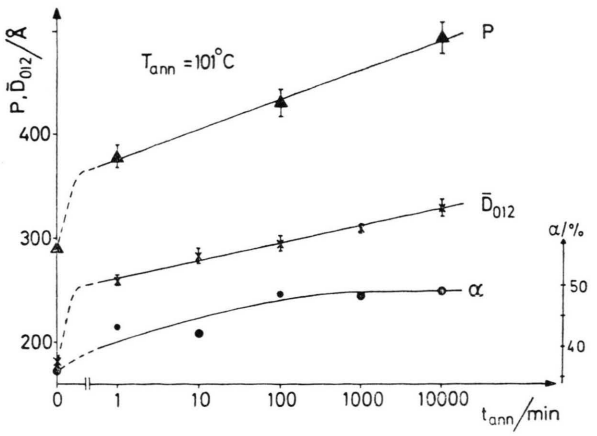

Fig. 7. Long period P, mean crystallite size in chain direction $\bar{D}_{012}$ and mean lateral crystallite size $\bar{D}_{110}$ of annealed samples of poly(1-butene) vs. the annealing time at an annealing temperature of 101 °C.

clearly in Fig. 6 near $T_{ann} = 110$ °C, but also near $T_{ann} = 80$ °C, where the mean size of the mPC's in chain direction has increased, but laterally is still the same. The temperature region up to about 85 °C has been called temperature range I [6]. In this range I no true melting occurs, but a "lateral melting" [7] of lamellae ends resulting in a slight and slow thickening neighbouring lamellae by solid state diffusion (see below). In temperature range II (85 °C—105 °C) melting and recrystallization starts and the lateral grain boundaries of neighbouring mPC's loosen up, so that the mPC's may grow together and scatter coherently. Altogether the lateral sizes as well as the lamellar thickness increase. In temperature range III (105 °C—115 °C) thickening occurs faster. But now in addition, permanently molten regions develop from which after quenching small mPC's recrystallize, the size of which corresponds to those of sample A in Figure 1. Beyond about 110 °C, therefore, the average $\bar{D}_{012}$ of all mPC's decreases rapidly.

b) Crystal Growth as Function of the Annealing Time

In Fig. 7 the crystallite size in chain direction, $\bar{D}_{012}$, as well as the long period P and the crystallinity α measured from DTA are plotted versus the annealing time at an annealing temperature of $T_{ann} = 101$ °C. Figure 7 shows effects already known from other semicrystalline polymers: A logarithmic increase of $\bar{D}_{012}$ and P with annealing time t_{ann} [30] and an increase of α. The crystallinity increases from 36% (quenched sample) to 48% for samples annealed more than about 100 min. Samples annealed at still higher temperatures also had a crystallinity of only about 50%.

There is a striking discrepancy between crystallinities measured by DTA, α_{DTA}, and those calculated from $\alpha_X = \bar{D}_{012}/P$ which are significantly higher as is seen from Table 6. In the case of polypropylene (PP) this discrepancy was explained by broad lateral grain boundaries between neighbouring mPC's in a lamella [31]. If β is the packing density of the mPC's within the lamellae, then

$$\alpha_{DTA} = \alpha_X \beta \tag{8}$$

holds. As seen from Table 6, β increases upon annealing from 0.59 to 0.73 compared with $\beta = 0.8$ in PP. This explanation is quite reasonable for PP, but not for PB, because in PP solely equatorial SAXS interferences between adjacent mPC's are observable. In PB on the other hand increases the

Table 6. Crystallinities of annealed samples of poly-(1-butene), mod. I measured by DTA, α_{DTA}, and X-rays, α_X as function of the annealing time in mod. II at an annealing temperature of 101 °C.

Annealing time [min]	α_{DTA} %	α_X %	$\beta = \alpha_{DTA}/\alpha_X$
0	36	61	0.59
1	43	69	0.62
10	42	—	—
100	48	69	0.70
1 000	48	—	—
10 000	49	67	0.73

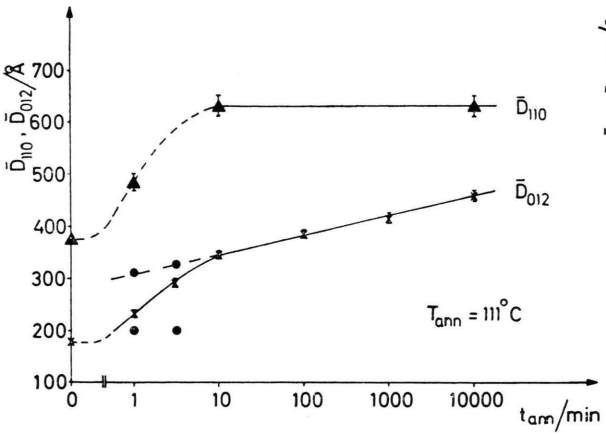

Fig. 8. Mean crystallite size in chain direction $\bar{D}_{012}$ and mean lateral crystallite size $\bar{D}_{110}$ of mod. II of poly-(1-butene) vs. the annealing time at an annealing temperature of 111 °C. The full circles were estimated from DTA (see text).

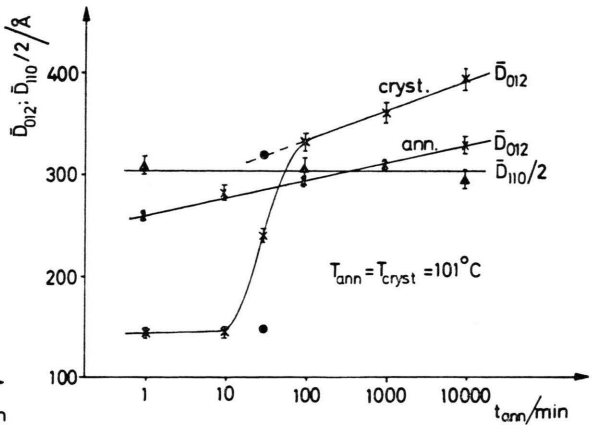

Fig. 9. Mean crystallite size in chain direction $\bar{D}_{012}$ and mean lateral crystallite size $\bar{D}_{110}$ of crystallized samples and of annealed mod. II of poly(1-butene), respectively vs. the crystallization and annealing time, respectively, at a crystallization and annealing temperature of 101 °C. The full circles were estimated from DTA (see text).

density of the amorphous phase appreciably with increasing annealing time as mentioned above (Figure 3). It is not understandable, why the DTA curve should solely depend on the heat of fusion of the mPC's, because the chain segments in the so called "amorphous phase" are also more and more fixed together with increasing annealing time. If moreover this contribution of heat of fusion concentrates also to smaller temperature intervals with rising annealing time (see Figure 4), then the difference between α_{DTA} and α_x may decrease, according to Table 6.

At an annealing temperature of 111 °C, there is an anomaly which could not be detected at 101 °C for annealing times greater than 1 min. In Fig. 8 the $\bar{D}_{012}$ for annealing times of 1 min and 3 min, no longer fits into the straight line through all the other measured values. The DTA curves of these two samples, on the other hand, show two peaks. The one at higher temperature originates from mPC's recrystallized at the annealing temperature of 111 °C, the other one at lower temperature has a T_m corresponding to samples quenched from the melt, i.e. a T_m approximately equal to that of sample A in Figure 1. The latter peaks correspond to molten percentages which could not recrystallize at the annealing temperature, but only after quenching. From the peak areas it is concluded that after 1 min annealing time only about 30%, after 3 min about 70% have recrystallized at the annealing temperature. Consequently the measured mean WAXS sizes "x" lie between the points "•" calculated from the DTA peaks and Figure 1. Within experimental error, the percentages recrystallized at 111 °C and 20 °C, respectively, measured by WAXS agree with those estimated from the DTA peak areas.

Raman investigations on PE crystallized for different times and afterwards quenched also revealed the existence of two different morphologies and have been explained in the same way [32]. The results in Fig. 8 show that the logarithmic increase of $\bar{D}_{012}$ with annealing time after complete recrystallization (DTA peak at lower temperatures disappears) can be only explained by a solid state diffusion. A comparison of Figs. 7 and 8 reveals an increase of the growth rate with rising annealing temperature [30].

As has been stated already, there is no correlation between the growth of the mPC's in chain direction and laterally. This clearly demonstrated by the results of Figs. 8 and 9, where $\bar{D}_{012}$ and $\bar{D}_{110}$ are plotted as function of the annealing time at $T_{ann} =$ 111 °C and $T_{ann} = 101$ °C, respectively. After complete recrystallization $\bar{D}_{110}$ stays constant whereas $\bar{D}_{012}$ shows a logarithmic increase with annealing time. This remarkable result reveals two things:

Firstly, the lateral growth of the mPC's during the first moments of annealing has obviously the same reason as the anomaleous increase of $\bar{D}_{012}$ at short annealing times (Figure 8). Its caused by

those quenched mPC's, which could not yet recrystallize. As soon as the recrystallization is complete, $\bar{D}_{110}$ remains the same upon prolonged annealing (cf. Figs. 8 and 9). If the recrystallization proceeds rapidly at relatively large supercooling, then $\bar{D}_{110}$ reaches its final value within the shortest annealing time (cf. Figure 9). The larger this value, the higher the annealing temperature (= recrystallization temperature) corresponding to a larger critical size of the seed. As mentioned above, possible rearrangements of neighbouring mPC's such that they scatter coherently [33], also lead to an increase of $\bar{D}_{110}$. Because of the enlarged chain mobility, this effect should also increase with rising temperature.

The second important conclusion is concerned with the way mPC's grow in chain direction. If single mPC's should refold, the increase of $\bar{D}_{012}$ should proceed at the expense of the lateral sizes, which has not been observed. Moreover, this process would require a tremendous rearrangement of the whole structure as there is no room left for the growing mPC's. Hence, the following two discontinuous steps of partial melting and recrystallization can easly explain the continuous increase of the mean values $\bar{P}$ and $\bar{D}_{012}$ with annealing time: i) Partial melting of mPC's at the ends of lamellae, ii) Cooperative refolding between the two neighbouring mPC's in chain direction. The refolding can proceed such that a whole mPC with an unprotected boundary is destroyed and one or both neighbouring mPC's in chain direction grow at its expense. This has been proved by Petermann et al. [26] by electron microscopy and corresponds exactly to the model given already in 1962 by Hosemann [7].

c) Crystal Growth During Recrystallization and Crystallization

As can be seen from Fig. 8, the growth of the mPC's also occurs during recrystallization upon annealing; the measured values ("•") fit exactly into the straight line which signalizes a logarithmic increase of $\bar{D}_{012}$ with t_{ann}, after complete recrystallization. The explanation of this behaviour during recrystallization is only possible by a solid state diffusion and supports our argumentation for the same process after complete recrystallization.

Not only during recrystallization upon annealing, but certainly also during crystallization from the melt, a thickening occurs as seen in Fig. 9 (curve "cryst") and which was shown for the first time by Hoffman and Weeks on PE [34]. Together with the $\bar{D}_{012}$-values measured on samples crystallized for different times at $T_{cryst} = 101\,°C$, the already known results of the annealing experiments at the same temperature are shown in Figure 9 (curve "ann"). Within experimental error the growth rates of $\bar{D}_{012}$ agree. Quite different, however, are the rates of crystallization and recrystallization, as is generally known. Recrystallization is complete (only one DTA peak) within an annealing time of 1 min, whereas crystallization ceases only after about 100 min.

Polydispersities

In Table 7 are listed the measured polydispersities g_D of the crystallite size mass-distribution in chain direction calculated from the 012-reflection profile for some samples. Above all there is a striking difference between the g_D-values of the quenched sample and of those annealed at 111 °C. The explanation is as follows: By quenching the sample from the melt to room temperature the crystallization takes place momentaneously at low temperature, where practically no crystal growth occurs. Upon annealing at 111 °C, however, the sample is melted partially and recrystallizes slowly. As soon as the seed has attained the critical size, it starts growing. As the recrystallization proceeds slowly and is complete only after 10 min of annealing time (cf. Fig. 8), the mPC's in the sample have different ages, i.e. markedly different sizes. The size distribution, therefore, is broader than for the quenched sample. This is shown directly by the plotted crystallite size mass-distribution of the quenched

Table 7. Mean crystallite size in chain direction $\bar{D}_{012}$ and the polydispersity g_D of the crystallite size mass-distribution in this direction of poly(1-butene) samples annealed for different times at different temperatures in mod. II.

Annealing time and temperature	$\bar{D}_{012}$ [Å]	g_D
0	150	0.16
24 h at 80 °C	231	0.21
24 h at 90 °C	270	0.21
24 h at 101 °C	316	0.27
1 min at 111 °C	233	0.50
100 min at 111 °C	386	0.41
10 000 min at 111 °C	460	0.40

sample and that of the sample annealed for 10^3 min at 111 °C in Figure 5. The distributions were calculated from the polydispersities g_d according to Eqs. (3) to (5). The relatively large value of $g_D = 0.50$ for the sample annealed for 1 min at 111 °C originates from the two different size distributions present in the sample around $\bar{D} =$ 313 Å and $\bar{D} = 201$ Å, which are reflected in the two DTA-peaks (see Figure 8).

Acknowledgement

We are grateful to Dr. G. Goldbach from Farbwerke Hüls. Without his help we would not have been able to prove our interpretation published in POLYMER 1962 on the increase of the long period and mean lamellae thickness during annealing and melting. With Prof. Dr. G. Yeh from the University Michigan we had some useful discussions with regard to the importance of mPC's for these phenomena.

[1] H.-G. Kilian, Kolloid-Z., Z. Polym. **231**, 534 (1969).
[2] I. R. Sanchez and R. K. Eby, J. Res. NBS **77 A 3**, 774 (1973).
[3] A. Peterlin, Polymer **6**, 25 (1965).
[4] H. Meyer and H.-G. Kilian, Colloid Polymer Sci. **64**, 166 (1978).
[5] E. W. Fischer, Kolloid-Z., Z. Polym. **218**, 97 (1967); **231**, 458 (1969).
[6] G. S. Y. Yeh, R. Hosemann, J. Loboda-Ćačković, and H. Čačković, Polymer **17**, 309 (1976).
[7] R. Hosemann, Polymer **3**, 349 (1962).
[8] J. Haase, R. Hosemann, and S. Köhler, Polymer **19**, 1358 (1978).
[9] G. Goldbach, Angew. Makromol. Chem. **29/30**, 213 (1973); **39**, 175 (1974).
[10] J. Boor and J. C. Mitchell, J. Polymer Sci. A **1**, 59 (1963).
[11] F. Danusso and G. Giannotti, Makromol. Chem. **88**, 149 (1965).
[12] G. Goldbach, DECHEMA-Fachausschuß Chemische Reaktionskinetik, Arbeitsausschuß Mehrphasensysteme, Frankfurt 1975.
[13] I. R. Rubin, J. Polymer Sci. B **2**, 747 (1964).
[14] A. Turner-Jones, J. Polymer Sci. B **1**, 455 (1963).
[15] B. Wunderlich, Macromol. Phys. Vol. **1**, Academic Press, New York 1973.
[16] H. Wilski and T. Grewer, J. Polymer Sci. C **6**, 33 (1964).
[17] W. Schmidt, Dissertation, TU Berlin 1975.
[18] J. Haase, R. Hosemann, and B. Renwanz, Colloid Polymer Sci. **255**, 849 (1977).
[19] R. Hosemann and W. Wilke, Markomol. Chem. **118**, 230 (1968).
[20] R. Hosemann, J. Polymer Sci. Symp. **50**, 265 (1975).
[21] R. Hosemann and S. N. Bagchi, Direct Analysis of Diffraction by Matter, North-Holland Publ. Comp., Amsterdam 1962.
[22] J. D. Hoffman, in: Treatise on Solid State Chemistry, Vol. 3, Plenum Press, New York 1976.
[23] J. Powers, J. D. Hoffman, J. J. Weeks, and F. A. Quinn, J. Res. NBS **69 A**, 335 (1965).
[24] G. Vidotto, D. Levy, and A. J. Kovacs, Kolloid-Z., Z. Polym. **230**, 289 (1969).
[25] J. L. Koenig and D. L. Tabb, J. Macromol. Sci. **B 9**, 141 (1974).
[26] J. Petermann, M. Miles, and H. Gleiter, J. Macromol. Sci. **B 12**, 393 (1976).
[27] N. Overbergh, H. Berghmans, and H. Reynaers, J. Polymer Sci. **14**, 1177 (1976).
[28] E. Ferracini, A. Ferrero, J. Loboda-Čačković, R. Hosemann, and H. Čačković, J. Macromol. Sci. **B 10** (1), 97 (1974).
[29] J. Loboda-Čačković and R. Hosemann, Colloid and Polymer Sci. (in press).
[30] E. W. Fischer, Pure Appl. Chem. **31**, 113 (1972).
[31] J. Loboda-Čačković, R. Hosemann, H. Čačković, A. Ferrero, and E. Ferracini, Polymer **17**, 303 (1976).
[32] J. Dlugosz, G. V. Fraser, A. Grubb, A. Keller, J. A. Odell, and P. L. Goggin, Polymer **17**, 471 (1976).
[33] H. Čačković, J. Loboda-Čačković, and R. Hosemann, J. Polymer Sci. Symp. **42**, 591 (1973).
[34] J. D. Hoffman and J. J. Weeks, J. Chem. Phys. **42**, 4301 (1965).